DETERMINATION OF CRACK TIP OPENING DISPLACEMENT OF CONCRETE BY EMBEDDED FIBER OPTIC SENSOR

Zhijun Zhang and Farhad Ansari
Department of Civil and Materials Engineering, University of Illinois at Chicago, Chicago, IL 60607 USA

ABSTRACT

Crack tip opening displacement (CTOD) is an important parameter that is often employed in characterization of fracture in engineering materials. Due to inherent difficulties in direct determination of CTOD, the crack mouth opening displacement (CMOD) has been measured during fracture tests of concrete beams and then related to CTOD. Analytical schemes are used for the determination of CTOD from the measured crack mouth opening displacements, which leads to the determination of other fracture parameters of importance. The research presented here describes development of an experimental technique for direct determination of CTOD based on embedded fiber optic sensors. The measured displacements, CTOD, and CMOD, are compared and the validity of analytical schemes in estimation of CTOD is evaluated.

1 INTRODUCTION

Crack tip opening displacement (CTOD) of concrete is significant in many ways. For instance, critical fracture may be assumed to occur when the crack-opening displacement exceeds a critical value. Moreover, CTOD embodies the constitutive properties of the micro cracked zone. It is difficult at best to experimentally determine the CTOD. Instead, CTOD is analytically related to the crack mouth opening displacement (CMOD), which is measured by a clip gauge extensometer or a linear variable differential transformer (LVDT). The interrelationship between CMOD and CTOD is complex mainly due to the considerable extent of the micro cracked zone in front of the crack tip.

Direct measurements of CTOD include using high resolution photography [1, 2] and fiber optic sensors [3, 4]. The former has limited applications and currently only suited for measurement of CTOD in thin metallic sheets. Optical fibers are small in diameter and can be embedded in concrete and therefore are good candidates for use as CTOD transducers. Ansari et al [3] and Lee et al [4] employed intensity and polarimetric type sensors for measurement of CTOD in concrete. The resolution of the intensity based sensor was too low for experiments involving monotonic tests. Interferometric techniques provide high-resolution measurements and they are perhaps the preferred method for measurement of CTOD [5]. However, these techniques require sophisticated instrumentation, such as an interferometer for the measurements.

The objective for the work presented here was to establish a simplified but high resolution speckle based fiber optic sensor embedded in concrete for the determination of CTOD. While detailed description of the optical method is beyond the scope of this article, a brief description of the sensor is provided for completeness.

2 FIBER OPTIC SENSING METHODOLOGY

Propagation of light in optical fibers is governed by the propagating modes traveling within the core of the fiber. The single mode fibers, with core diameter between 5 to 9 microns, carry only a single signal pertaining to the first mode of propagation. Multimode fibers, on the other hand, carry several modes due to the larger diameter cores ranging from 50 to 62.5 microns. The effect of modes on the intensity of the signal is the speckled appearance of the light exiting the fiber end. Straining or

deforming the fiber perturbs the propagation of the modes and the pattern of the speckles within the field (Fig.1). This attribute can be utilized for construction of a simple sensor, provided that the speckle intensity varies linearly with strain. The transduction mechanism is based on the correlation between the applied strain to the fiber and the light intensity variation of speckle patterns due to mode redistribution in a multimode fiber.

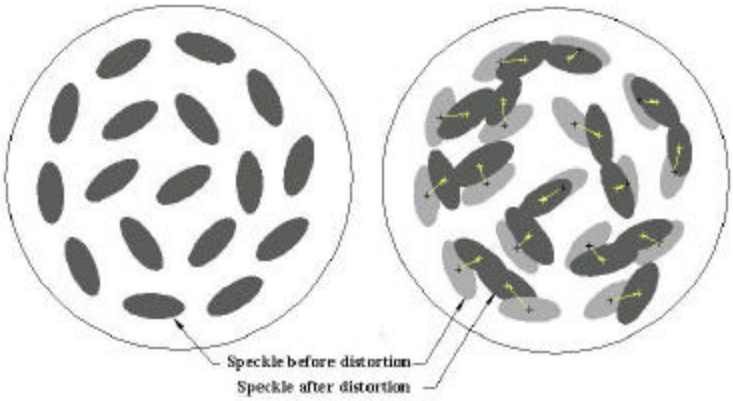

Figure 1: Schematic representation of mode redistribution within a speckle field

The variation in the propagating modes within the speckle pattern is described by the normalized speckle intensity variations, (*SIV*) over the whole speckle field

$$\Psi_n = \frac{\iint_S |\Delta I| dxdy}{\iint_S I dxdy} \propto d(\Delta b_{ml} L) \tag{1}$$

Where Ψ_n is the normalized *SIV*, $\iint_S I dxdy$ is a constant and it is the integrated intensity of the speckle field within the cross section of the optical fiber in the *x-y* coordinate system, ΔI is the change in the spatial intensity, Δb_{ml} is the difference in the propagation constants between the *m* th and *l* th modes, and L is the gauge length of the optical fiber. ΔI is proportional to $d(\Delta b_{ml} L)$ which is the phase variation due to the external perturbation change, i.e. strain. The variation from one state to another is given by

$$d(\Delta b_{ml} L) = C_{ml} L n_{eff} e \tag{2}$$

Where

$$n_{eff} = n\{1 - \frac{1}{2} n^2 [p_{12}(1 - n) - p_{11} n]\} \tag{3}$$

n is the refractive index of the glass core of the optical fiber, $e = \frac{dL}{L}$ is the applied strain which alters both the fiber length and the local index of refraction (photo elastic effect), p_{11}, and p_{12} are the Pockel's constants related to the photo elastic effects in the optical fiber. C_{ml} is a proportionality constant corresponding to the *m* th and *l* th modes. Proportionality between the change in the propagation modes and the strain is only valid over a very small range of Le . i.e. the dynamic range of the sensor is small. A video camera attached to an image capture board is employed for acquisition of speckle

patterns from the output end of the fiber. Image data is then numerically evaluated for the computation of *SIV* according to eqn (1). Exhaustive description of the method including the numerical computations is given elsewhere by Spillman et al [6] and Pan et al [7].

3 EXPERIMENTS AND ANALYSIS

The experimental program included calibration and experimentation with concrete beams. The purpose for calibration was to develop a relationship between *SIV* and the induced deformations. The calibration procedure was designed to measure the strain over the three different gauge lengths of 25, 50, and 75 mm. This procedure allowed for assessment of sensitivity and dynamic range for the individual gauge lengths considered in this study. The sensors with varying gauge length were later employed in the three-point bending tests and the results were analyzed and compared with the estimated CTOD from the measured CMOD.

3.1 Calibration

Calibration tests involved point loading of the plexi glass cantilever beam shown in Fig.2. The beam had a cross section of 24mm x 6 mm and a span length of 320 mm. Fig.3 corresponds to the calibration test results in terms of *SIV* as a function of strain. The calibration results were repeatable and linear with coefficients of correlation varying between 0.97 and 0.99. Other parameters of importance including sensitivity in terms of displacements and the dynamic range for the three calibrated gauge lengths are given in table 1.

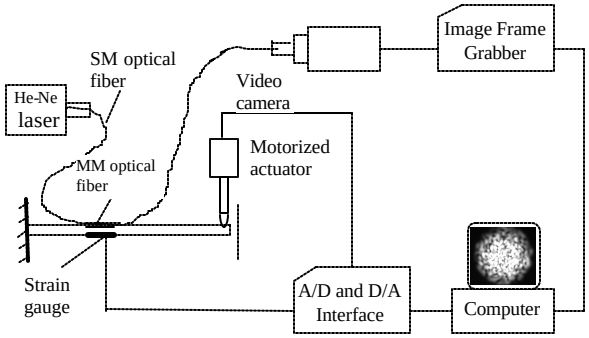

Figure 2: Cantilever beam calibration test setup

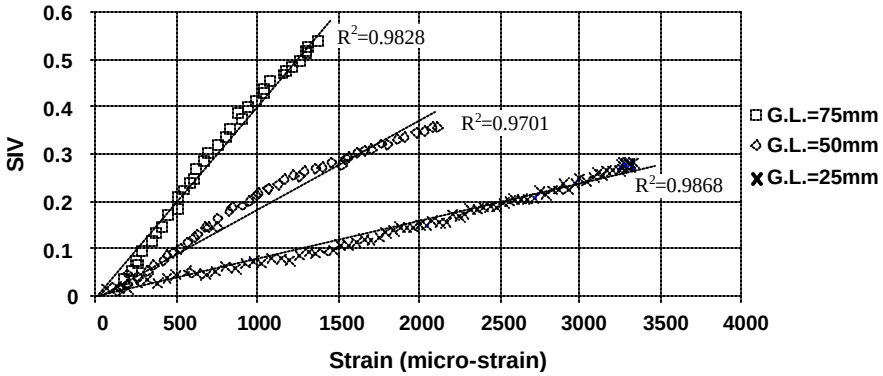

Figure 3: Cantilever Beam calibration test results

Table 1: Characteristics of the optical fiber sensors

Gauge Length (mm)	25	50	75
Sensitivity (SIV/Micron)	$3.26X10^{-3}$	$3.53X10^{-3}$	$6.02X10^{-3}$
Dynamic Range (in micro-strain)	3200	2000	1200

3.2 CTOD Measurements in Concrete

A single mode fiber was spliced to the multimode fiber in front of the crack tip. The multimode fiber of gauge length was embedded 3 mm ahead of the notch tip, and the lead out section of the multimode fiber was bent out of the plane of loading to exit the beam. The lead out section of the multimode fiber was then shielded with petroleum jelly, which is a simple effective damper for this purpose.

The schematic diagram for the experimental setup is shown in Fig.4. The center edge notched concrete beams had dimensions of 10cm×10cm×86cm and a notch depth of 5 cm. Total six beams have been tested.

3.3 Experimental Results and analysis

Typical load versus measured CMOD and CTOD result is shown in Fig.5. The measured critical CTOD and CMOD results for all of the specimens are given in table 2. Some data for beams B03 and B06 are not reported due to the malfunction of the LVDT.

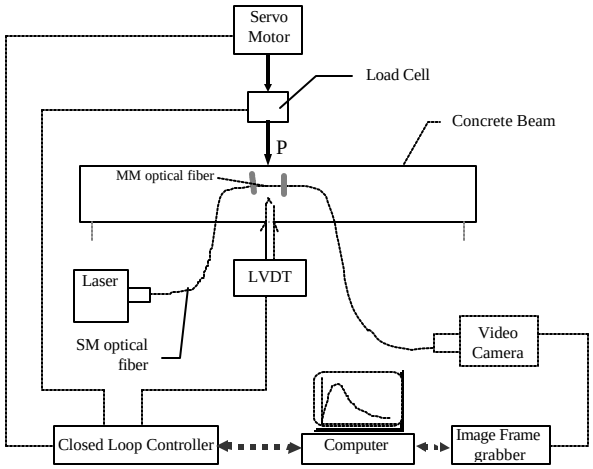

Figure 4: Three-point bend beam test setup

Table 2: Measured and computed crack opening displacements

Specimen	Peak load (N)	Effective crack length at peak load a_c (mm)	Measured $CTOD_c$ (micron)	Calculated $CTOD_c$ (micron)	Measured $CMOD_c$ (micron)
B01	644.59	72.72	31.14	29.60	76.35
B02	542.58	76.40	36.45	36.47	89.70
B03	551.64		36.11		
B04	448.57	79.18	33.31	40.40	96.40
B05	444.13	76.86	36.90	39.52	94.37
B06	461.83		37.53		

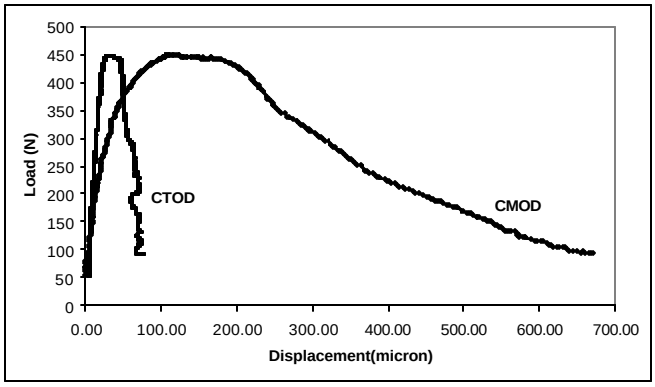

Figure 5: Typical measured CMOD and CTOD responses of the concrete beam

To evaluate the validity of such methods, an effective-elastic crack approach is employed for computation of CTOD, effective crack length, and comparison of the computed values with the experimental results. The effective-elastic crack approach uses the Griffith-Irwin fracture energy dissipation mechanism and models the fracture process zone by employing an equivalent, traction-free elastic crack. The CTOD could be calculated with the combination of the following equations [8]:

$$CMOD = \frac{4s\,a}{E} g_1\left(\frac{a}{b}\right) \tag{4}$$

$$CTOD = CMOD\, g_2\left(\frac{a}{b}, \frac{a_0}{a}\right) \tag{5}$$

$$s = \frac{3PS}{2b^2 t} \tag{6}$$

Where, s is tensile stress at the crack tip, P is the load, S is the span length, b is the width, and t is the depth of the beam, a_0 is the initial notch length, and a is the effective elastic crack length. The functions g_1 and g_2 are related to geometric dimensions of the beams and for the beams studied here (S/b=6.0), they were estimated by interpolation with those for S/b = 4 and pure bending [8]. The modulus of elasticity E can be determined through the method proposed by RILEM [9]:

$$E = \frac{6Sa_0 g_1\left(\frac{a_0}{b}\right)}{C_i b^2 t} \tag{7}$$

Where C_i is the initial compliance determined from Load-CMOD curve.

The computed critical CTOD and effective crack lengths are included in Table 2, and the crack opening displacements are compared with the experimentally determined values. As shown in Table 2, there is a close agreement between the computed and the measured values of critical CTODs. The computed and measured crack opening displacements for two extreme cases are further compared in Fig.6. As shown in the load–CTOD responses, while one of the beams exhibited an almost perfect match between the computed and measured crack opening displacements, the other did not, except for the peak value. The match between the computed and measured pre peak load-CTOD response for other specimens fall somewhere in between the two extreme cases.

4 CONCLUSIONS

Development and testing of a fiber optic CTOD sensor for embedment in cementitious composites has been described. The sensor principle is based on propagation mode intensity modulations in the

speckle patterns generated in multi mode optical fibers. The instrumentation includes a communication grade multi mode optical fiber, a laser with a wavelength in the visible range of the spectrum, and a digital video camera. The sensor has a high signal to noise ratio and is very sensitive with displacement measurement capability in the micron level.

The measured crack tip opening displacements with the proposed fiber optic sensor were compared with analytical results and in general the measured and computed values of critical CTOD were in agreement. On average, all the specimens exhibited the same level of critical crack tip opening displacements. The potential exists for determination of the entire process zone length through embedment of several such sensors in the micro cracked zone through multiplexing schemes. More research is needed to further study the displacements within the process zone.

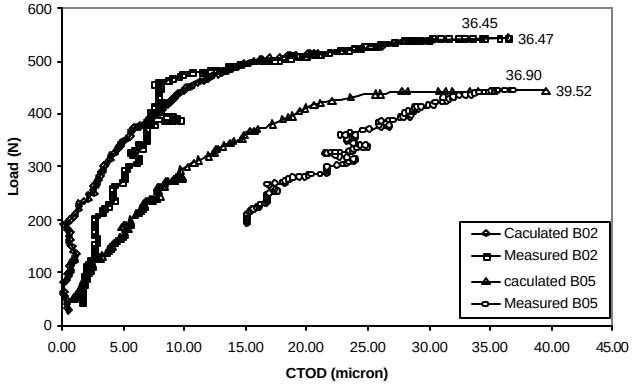

Figure 6: Comparison of measured and calculated CTOD for beams B02 and B05

REFERENCES

[1] Dawicke DS, Sutton MA. CTOA and crack tunneling measurements in thin sheet 20240T3 aluminum alloy. Exp Mech. 34(4):357; 1994.

[2] Dawicke DS, Newman Jr JC, Bigelow CA. Three dimensional CTOA and constraint effects during stable tearing in a thin-sheet material. ASTM STP. 1256:223-242; 1995.

[3] Ansari F, Navalurkar R. Kinetics of crack formation in cementitious composites by fiber optics. ASCE, J. of Engineering Mechanics. 119(5):1048-1061; 1993.

[4] Lee I, Libo Y, Ansari F, Ding H. Fiber optics crack tip opening displacement sensor for concrete. Cement and Concrete Composites. 19(1):59-68; 1997.

[5] Yuan L., Ansari F. Embedded white light interferometer Fibre optic strain sensor for monitoring crack-tip opening in concrete beams. Meas. Sci. Technol. (9):261-266; 1998.

[6] Spillman WB, Kline BR. Statistical-mode sensor for fiber optic vibration sensing uses. Applied Optics. 28(15):3166-3176; 1989.

[7] Pan K, Uang C, Cheng F, Yu F. Multimode fiber sensing by using mean-absolute speckle-intensity variation. Applied Optics. 33(10):2095-2098; 1994.

[8] Tada H, Paris PC, Irwin GR. The stress analysis of crack handbook. 3rd ed.; ASME Press, New York, NY, 2000.

[9] RILEM Technical Committee 89-FMT (1990). Determination of fracture parameters (K^s_{IC} and $CTOD_c$) of plain concrete using three-point bend tests, proposed RILEM draft recommendations. RILEM, Materials and Structures. 23(138): 457-460.